

Greener Synthesis of Nano Hydroxyapatite using Fatty acids template for the application of Tissue Engineering Nano Hydroxyapatite: Fatty acids Synthesis and Characterizations

Sumathra Murugan and Mariappan Rajan*

Department of Natural Products Chemistry, School of Chemistry, Madurai Kamaraj University, Madurai, India

*Corresponding author: Mariappan Rajan, Department of Natural Products Chemistry, School of Chemistry, Madurai Kamaraj University, Madurai - 625021, India, Tel: +919488014084; E-mail: rajanm153@gmail.com

Received date: 11 July, 2017; Accepted date: 10 August, 2017; Published date: 15 August, 2017

Copyright: © 2017 Murugan S, et al. This is an open-access article distributed under the terms of the Creative Commons Attribution License, which permits unrestricted use, distribution, and reproduction in any medium, provided the original author and source are credited.

Abstract

Nano-hydroxyapatite (nano-HAp) is significant import as a bio-ceramic material for use in orthopedic applications because of its comparability in size, crystallography and substance creation with human hard tissue. In this present study, the biologically high interest of nano-HAp was synthesized as green template mode approaches using the various fatty acids like linoleic acid, lauric acid, and oleic acid. The influence of the fatty acid for the formations nano-HAp structure and nature of fatty acid during synthesis was investigated. The nano-HAp functionality, crystallinity, and morphology were determined by FTIR, XRD, and SEM techniques, respectively. The biocompatibility of HAp on MG63 cell line was confirmed by *in vitro* MTT assay method. The *in-vitro* studies showed better biocompatibility and cell proliferation results on the template assist synthesized nHAP. These results indicate that nHAp form the green methodology could be a promising material for bone tissue engineering.

Keywords: Green synthesis; Fatty acids; Hydroxyapatite; Template; Tissue engineering

Introduction

Every year, millions of patients suffer from bone fractures resulting from natural disasters, traffic accidents, population aging, and so on. The need for bone substitutes to replace/restore the function of damaged/lost bone has become a major clinical challenge [1,2]. Current research, serious advances have been accomplished to treat the difficulty or displeasure of bone implant materials with cell/tissues based tissue engineering. Bone implant materials must be considered accompanying the criteria of morphology, structure, porosity of the materials, acceptable mechanical superiority, biocompatibility and biodegradability [3]. Hydroxyapatite is the chief materials used for the artificial dental and bone implantation applications [4]. Hydroxyapatite (HAp) is of high importance in material research and pharmaceutical applications as they constitute of the major inorganic portion of human hard tissues like bone and teeth [5,6]. It has been broadly expected for the utilizations of bone substitution, dental distortion satisfying, and bone tissue designing and bioactive carriers because of its excellent biocompatibility, bioactivity, absorbability, osteoconductivity, mechanical property and rich surface properties [7-10]. Hence, some researchers have attempted to synthesis HAp nanoparticles with a unique attention. Nano particles HAp (Nano HAp) can imitate the measurements of the constituent segments of regular tissues which improve the osteoblasts attachment and resorption of long haul tissue designed inserts [11-13]. Additionally, the layout option is a standout amongst the most adaptable and helpful technique, as it is exceptionally powerful in delivering particles having the size in the scope of nanometers together with a limited level of agglomeration and a controlled morphology [14,15]. Nanoparticles with specific sizes and morphologies can be readily synthesized by a variety of methods. The recent research has been focused on the

synthesis of nanoparticles by green template method using eco-friendly natural sources as the template material [16]. The synthesis of nanomaterial with using template systems has an important technique for the production nanomaterial as controlled sizes. In recent years many researchers have tried to synthesize nanoparticles with the naturally abundant green materials since they are renewable, cost-effective and environmentally benign when compared to other synthetic organic templates [17-19]. Focusing of natural biological materials contains carbohydrates, proteins, fibers and polysaccharides peptides, nucleic acids and fatty acids in significant amounts. The nanosized hydroxyapatite obtained from this method with structural features has close to those of biological apatites that make them attractive for bone tissue engineering applications. In this present study, we have investigated the formation of HAp by using various fatty acids as a template and the fatty acid is varied with a number of carbon and saturation of the carbon atoms. For the formation of HAp, such fatty acid the general function group of carboxyl can promote the binding of calcium ions (Ca_2^+) from the solution of carboxylate ions. This initiates the crystal nucleation and growth and thus helps in HAp thereby promoting size controlled formations [20,21]. This work was established the enhancement of morphology, purity, and crystalline behavior of HAp nanoparticles was performed for bone engineering applications.

Materials and Methods

Materials

Calcium chloride dihydrate ($\text{CaCl}_2 \cdot 2\text{H}_2\text{O}$), diammonium hydrogen phosphate ($(\text{NH}_4)_2\text{HPO}_4$), ethanol, toluene, liquid ammonia, Lauric acid, linoleic acid and Oleic acid were received from Sigma-Aldrich, Egmore, Chennai, India. Analytical grade chemicals were used throughout experiments without any further refinements. The double distilled (DD) water was used throughout experiments.

Preparation of HAP nanoparticles

The typical synthetic procedure for the preparation of HAP nanoparticles is as follows 5 mL of deionized water, 5 mL of ethanol and 5 mL of oleic acid were mixed under stirring for five minutes. 10 mL of an aqueous solution containing $\text{CaCl}_2 \cdot 2\text{H}_2\text{O}$ (0.05 M) was added drop wise into the above ternary solvent system, and 10 min later, 10 mL of an aqueous solution containing 0.03 M $((\text{NH}_4)_2\text{HPO}_4)$ was added drop wise. The pH of the reaction solution was sustained at pH 10.0 by using aqueous ammonia and the stirring was elongate to about 24 h. The resultant product was washed thrice with water followed by ethanol and then dried at 40°C. Followed by the synthesized composite was sintered for 12 h at 850°C in a muffle furnace to remove the template of fatty acid to obtain HAP nanoparticles. Similarly, the synthesis of nanoparticles was carried out in the Linoleic acid and Lauric acid by the inside of oleic acid.

Characterization of HAP

Fourier transforms infrared spectroscopy (FTIR) The nanoHAP were characterized using a Bruker tensor 27 series FTIR spectrometer in the region of 400-4000 cm^{-1} with 2 cm^{-1} resolution and 16 scans. The test samples were prepared by mixing 0.2 g sample powder together with 1 g KBr to make a pellet using a hand press.

X-ray Diffraction The X-ray diffraction (XRD) analysis was carried out to investigate the phase composition and crystallinity of as-synthesized HAP nanoparticles and its composites. This analysis was performed in a Bruker D8 Advance Diffractometer with monochromatic Cu K α source operated at 40 kV and 30 mA. An acceleration voltage of 30 kV and a current of 15 mA were used. The analysis was performed over the 2 θ range of 10 to 60° in step scan mode with a size of 0.02° and at a scan rate of 0.02°/min.

Field emission scanning electron microscopy (FESEM) The morphology and microstructure of then nHAP were examined using FESEM (VEGA3 TESCAN) operated at an accelerating voltage of 10 kV equipped with energy dispersive X-ray analysis (EDAX).

Cell culture and *in vitro* cell viability

Osteoblast MG-63 cells were cultured in Dulbecco's modified Eagle's medium (DMEM) supplied with 10% fetal bovine serum (FBS) and 1% penicillin-streptomycin at 37°C under a 5% CO_2 humidified atmosphere for 24 h and used for the cell viability test. And the prepared HAP nanoparticles were sterilized by UV light treatment for 20 min and put into the culture well plate for the cell viability test. The cells were seeded in a 96-well micro assay plate in a concentration of 1×10^4 cells per well, then the sterilized HAP microtubes were added to the wells at a concentration ranging from 0.1 to 100 $\mu\text{g mL}^{-1}$ and cultured with the cells for 24 h. Finally, cell viability was quantified by the 3-(4,5-dimethyl-thiazol-2-yl)-2,5-diphenyltetrazolium bromide (MTT) assay. After incubated for 1, 3, and 7 days, the sample solution was removed and 100 μL MTT solution (5 mg/mL) was added in 1mL culture medium to each well and then incubated at 37°C for 4h. Thereafter, 1mL dimethylsulfoxide (DMSO) was added after the supernatant medium was removed. Finally, the solution was centrifuged to remove the nano-HAP before transferred into the 96-well plate and the absorbency value (OD value) was recorded at a wave length of 490 nm.

Statistical analysis

All experiments were repeated independently and triplicated. Statistical analysis was accomplished by using one-way analysis of variance (ANOVA). When the overall ANOVA Ftest was analysed using Tukey's test for a post hoc comparison. Data are reported as mean \pm standard deviations (SD) with a significance level of $P < 0.05$.

Results and Discussion

FT-IR analysis

The formation of nano-HAP by the assistance of three different fatty acids, such as Lauric acid, linoleic acid, and Oleic acid was characterized their functionality. The identification of functional groups in nano-HAP was analyzed by Fourier transform spectroscopy (Figure 1). The FTIR spectrum of formed HAP by the assistance of Lauric acid and linoleic acid was presented in Figure 1a and 1b. The FTIR results indicate that the some of the peaks positions and intensity of the corresponding HAP were absent Figure 1a and 1b. Another visible difference regards the band 500 to 1300 cm^{-1} shows that the intensity of the peaks decreased with the formation of HAP by the Lauric acid and linoleic acid. The FTIR spectra Figure 1c demonstrate the peaks at 573, 595, 964, 1034, 1091 cm^{-1} attributed to the PO_4^{3-} a group of nano-HAP. The peak at 3633 cm^{-1} derives from the hydroxyl group in nano-HAP synthesized in the template of oleic acid. The FTIR result of Figure 1c confirms the formation of HAP by the assistance of oleic acid. The main influence in the formation of HAP was rolled by the chain length. The oleic and linoleic acid have same chain length, in this category; the unsaturation of carbon atom has controlled the formation of nano-HAP [22,23].

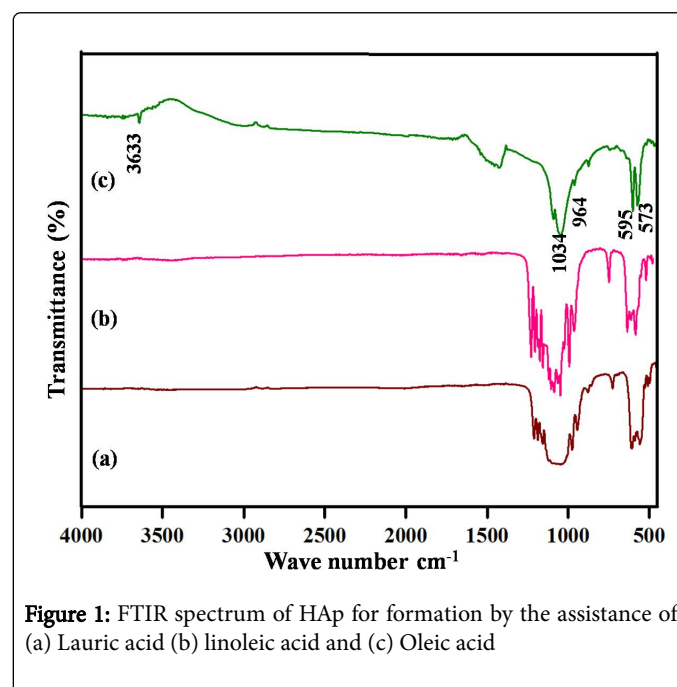


Figure 1: FTIR spectrum of HAP for formation by the assistance of (a) Lauric acid (b) linoleic acid and (c) Oleic acid

XRD studies

XRD patterns of the nano-HAP synthesized by the influence of Lauric acid, linoleic acid, and Oleic acid. For all the XRD patterns, the representative diffraction peaks of hexagonal $\text{Ca}_{10}(\text{PO}_4)_6(\text{OH})_2$ were

distinguished, which can be indicated conforming to the standard data of JCPDS No. 09-0432 [21,22]. The corresponding characteristic peaks at 26,32,33,40 attributed to (002), (211), (300), and (310) planes respectively shown in Figure 2c. Based on this observation, the crystalline structure of nano-HAp was established by the green way synthesis. It is essential to that the template synthesis of different fatty acids change the crystallinity and morphology of the nanomaterials, as the varieties of the crystallinity can be completely attributed to the varieties in the nano-topography of the materials and low crystallinity will be promoting the biological improvements. In addition, Lauric acid and Linoleic acid was significant decreases the intensity and crystalline nature of the synthesized nano-HAp shown in Figure 2a and 2b. This indicates the acids were not able to influence the complete formation of HAp. The XRD pattern again reveals the formation of nano-HAp along with tricalcium phosphate.

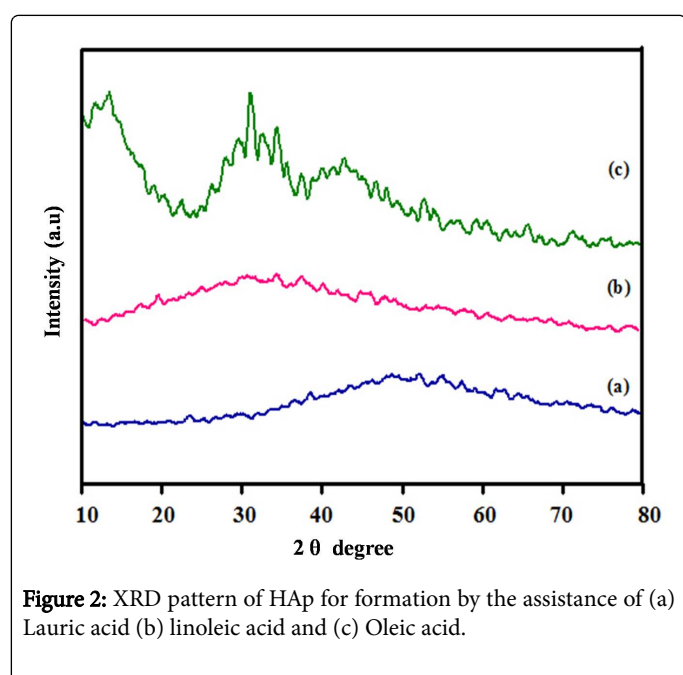


Figure 2: XRD pattern of HAp for formation by the assistance of (a) Lauric acid (b) linoleic acid and (c) Oleic acid.

Surface morphology

The SEM images show that the HAp has particles structure. The fatty acids control the morphology of the particles size and structure. The particles morphology was changed in different fatty acids such as Lauric acid, linoleic acid, and Oleic acid Figure 3a-3c. The spherical particles occurred in the oleic acid as a template, it is due to the cross linking between the fatty acid chains carboxylate group and Ca_2+ Figure 3c. The EDAX spectra for the HAp synthesized using oleic acid is shown in Figure 3d. EDAX spectrum indicates the mineral composition of nano-HAp and purity of the HAp [24].

Cell viability

In Figure 4a MG63 cells, can be a high biocompatibility of HAp composite might be clarified by the properties of as-incorporated nano-HAp from oleic acid with green way process. In Figure 4a results indicate that the as-synthesized nano-HAp has favorable properties for the adhesion and proliferation of MG63 cells. In Figure 4a the arrow indicates the filopodia of the MG63 cells were increased after 3d, 7d, in the presence of nano-HAp materials, which are the typical morphological features of osteoblasts.

The compatibility of MG63 cells regarded with the asincorporated samples of HAp appears in Figure 4b. The viability of nano-HAp and control cells was measured by MTT assay method. The results of the MTT assay revealed that MG63 cells proliferated when treated with the as-synthesized samples and the control when the culture duration was extended from 1d, 3d, and 7d. The reasonability of HAp synthesized from oleic acid helped the development of treated with MG63 cell lines and control cells were measured. The outcomes demonstrate that MG63 cells can multiply within the sight of the nano-HAp showing that the material is biocompatible.

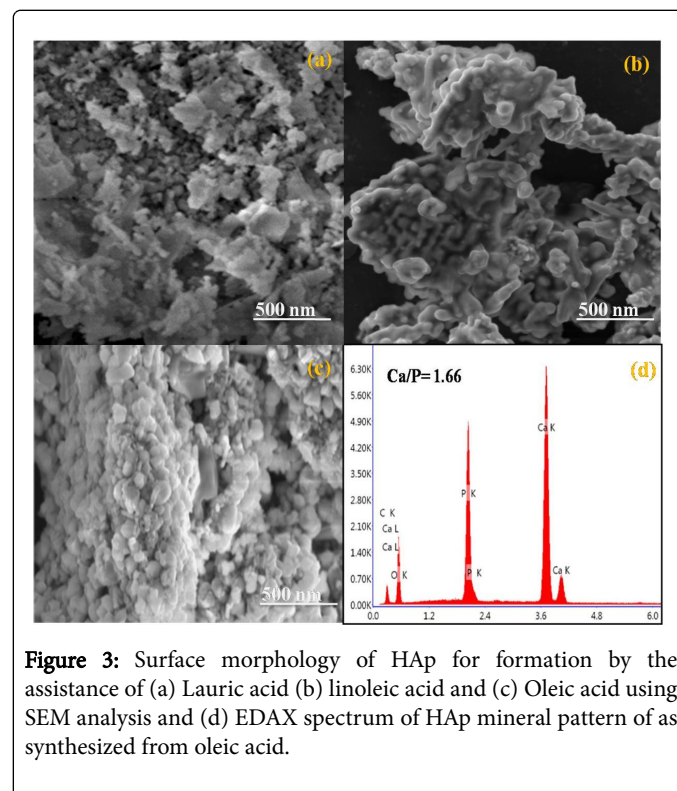
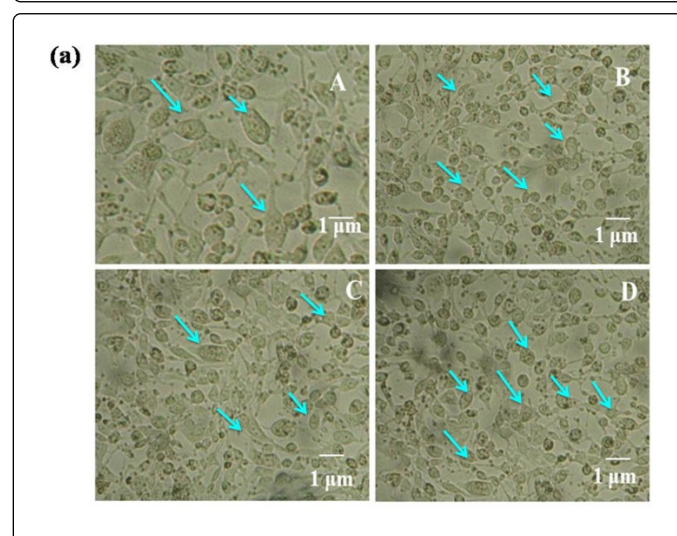


Figure 3: Surface morphology of HAp for formation by the assistance of (a) Lauric acid (b) linoleic acid and (c) Oleic acid using SEM analysis and (d) EDAX spectrum of HAp mineral pattern of as synthesized from oleic acid.



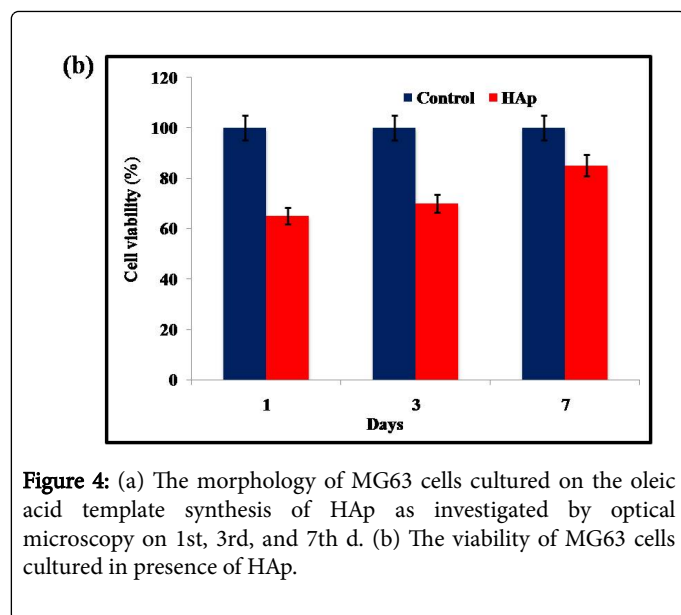


Figure 4: (a) The morphology of MG63 cells cultured on the oleic acid template synthesis of HAp as investigated by optical microscopy on 1st, 3rd, and 7th d. (b) The viability of MG63 cells cultured in presence of HAp.

Conclusion

We have established the synthesis of nano hydroxyapatite using three different fatty acids namely oleic acid, linoleic acid and lauric acid as a template. We are concluded that the nature of the fatty acid was found an impact on the HAp nanoparticles formations as functionality and crystallinity and it is well evidenced by the from FTIR and XRD respectively. The SEM images demonstrated that fatty acid plays a major role on the controlling as well as reducing the size of nanoparticles. At the oleic acid system, HAp nanoparticles showed the smallest particle size and spherical nature. The as-synthesized nano-HAp particles prepared using natural fatty acid possesses excellent bioactivity and biocompatibility along with a strong cell adhesion activity against MG63 and it is making them potential materials for tissue engineering, orthopedic, and dental applications.

Acknowledgment

MR received financial support from the Department of Science and Technology, Science and Engineering Research Board (Ref: YSS/2015/001532; New Delhi, India) and the University Grants Commission (UGC), Government of India, under the "UGC-MRP" plan (F.No.-43- 187/2014 (SR), and from the PURSE program for the purchase of the SEM and FT-IR equipment.

References

- Liu XH, Smith LA, Hu J, Ma PX (2009) Biomimetic nanofibrous gelatin/apatite composite scaffolds for bone tissue engineering. *Biomaterials* 30: 2252-2258.
- Katti KS (2006) Why is nacre so tough and strong? *Mater Sci Eng C* 26: 1317-1324.
- Verma D, Katti KS, Katti DR (2008) Effect of Biopolymers on Structure of Hydroxyapatite and Interfacial Interactions in Biomimetically Synthesized Hydroxyapatite/Biopolymer Nanocomposites. *Ann Biomed Eng* 36: 1024-1032.
- Rodríguez-Navarro AB, CabraldeMelo C, Batista N, Morimoto N, Alvarez-Lloret P, et al. (2006) Microstructure and crystallographic-texture of giant barnacle (*Austromegabalanus psittacus*) shell. *J Struct Biol* 156: 355-362.
- Weiner S, Addadi L (1997) Design strategies in mineralized biological materials. *J Mater Chem* 7: 689-702.
- Aoki H (1991) Science and Medical Applications of Hydroxyapatite. Japanese Association of Apatite Science, Takayama Press System Centre Co. Inc., Tokyo, Japan. 179-192.
- Hench LL (1991) Bioceramics: From Concept to Clinic. *J Am Ceram Soc* 74: 1487-1510.
- Navarro M, Michiradi A, Castano O, Planell JA (2008) Biomaterials in orthopaedics. *J R Soc Interface* 5: 1137- 1158.
- Viswanath B, Ravishankar N (2008) Controlled synthesis of plate-sHAPed hydroxyapatite and implications for the morphology of the apatite phase in bone. *Biomaterials* 29: 4855-4863.
- Rey C, Combes C, Drouet C, Sfihi H, Barroug A (2007) Physico-chemical properties of nanocrystalline apatites: Implications for biominerals and biomaterials. 27: 198-205.
- Agrawal K, Singh G, Puri D, Prakash S (2011) Synthesis and Characterization of Hydroxyapatite Powder by Sol-Gel Method for Biomedical Application. 10: 727-734.
- Shinto H, Hirata T, Fukasawa T, Fujii S, Maeda H, et al. (2013) Effect of interfacial serum proteins on melanoma cell adhesion to biodegradable poly(L-lactic acid) microspheres coated with hydroxyapatite. *Colloids Surf B Biointerfaces* 108: 8-15.
- Ito Y, Hasuda H, Kamitakahara M, Ohtsuki C, Tanihara M, et al. (2005) A Composite of Hydroxyapatite with Electro-spun Biodegradable Nanofibers as a Tissue Engineering Material. *Journal of bioscience and bioengineering*, 100: 43-49.
- Shanthi PM, Mangalaraja RV, Uthirakumar AP, Velmathi S, Balasubramanian T, et al. (2010) Synthesis and characterization of porous shell-like nano hydroxyapatite using Cetrinide as template. *J Colloid Interface Sci* 350: 39-43.
- Klinkaewnarong J, Swatsitang E, Masingboon C, Seraphin S, Maensiri S (2010) Synthesis and characterization of nanocrystalline HAp powders prepared by using aloe vera plant extracted solution. *Curr Appl Phys* 10: 521-525.
- Fang W, Zhang H, Yin J, Yang B, Zhang Y, et al. (2016) Hydroxyapatite Crystal Formation in the Presence of Polysaccharide. *Cryst Growth Des* 16: 1247-1255.
- Patil RS, Kokate MR, Kolekar SS (2012) Bioinspired synthesis of highly stabilized silver nanoparticles using *ocimum tenuiflorum* leaf extract and their antibacterial activity. *Spectrochim Acta A* 91: 234-238.
- Rao YS, Kotakadi VS, Prasad TNVKV, Reddy AV, Gopal DVRS (2013) Green synthesis and spectral characterization of silver nanoparticles from lakshmi tulasi (*Ocimum sanctum*) leaf extract. *Spectrochim Acta A Mol Biomol Spectrosc* 103: 156-159.
- Bankar A, Joshi B, Kumar AR, Zinjarde S (2010) Banana peel extract mediated synthesis of gold nanoparticles. *Colloids Surf B Biointerfaces* 80: 45-50.
- Wu F, Lin DDW, Chang JH, Fischbach C, Estroff LA, Gourdon D (2015) Effect of the Materials Properties of Hydroxyapatite Nanoparticles on Fibronectin Deposition and Conformation. *Cryst Growth Des* 15: 2452-2460.
- Sumathra M, Govindaraj D, Jeyaraj M, Al Arfajc A, Munusamy MA, et al. (2017) Sustainable pectin fascinating hydroxyapatite nanocomposite scaffolds to enhance tissue regeneration. *Sustainable Chemistry and Pharmacy* 5: 46-53.
- Areias AC, Ribeiro C, Sencadas V, Garcia-Girat NV, Diez-Perez A, et al. (2012) Influence of crystallinity and fiber orientation on hydrophobicity and biological response of poly(L-lactide) electrospun mats. *Soft Matter* 8: 5818-5825.
- Phan BTN, Nguyen HT, Dao HQ, Pham LV, Quan TT, et al. (2017) Synthesis and characterization of nano-hydroxyapatite in maltodextrin matrix. *Appl nanosci* 7: 1-7.
- Khandelwal H, Prakash S (2016) Synthesis and Characterization of Hydroxyapatite Powder by Eggshell. *Journal of Minerals and Materials Characterization and Engineering* 4: 119-126.